Mapping woody plant cover in desert grasslands using canopy reflectance modeling and MISR data

Mark J. Chopping,[1] Lihong Su,[1] Andrea Laliberte,[2] Albert Rango,[2] Debra P. C. Peters,[2] and John V. Martonchik[3]

Received 7 June 2006; revised 26 July 2006; accepted 31 July 2006; published 9 September 2006.

[1] A simplified geometric-optical model (SGM) was inverted using red band reflectance data acquired at 275 m in nine viewing angles from the Multiangle Imaging SpectroRadiometer (MISR) flown on NASA's Terra satellite, to provide estimates of fractional woody plant cover for large areas (over 3519 km^2) in parts of the Chihuahuan Desert in New Mexico, USA. The use of the model in these semi-arid environments was enabled by the derivation of *a priori* estimates of the soil/understory background reflectance response. This was made possible by determining relationships between the kernel weights from a LiSparse-RossThin model adjusted against the same MISR data – together with spectral reflectance data derived from MISR's nadir-viewing camera – and the parameters of the Walthall model used to represent the background. Spatial distributions of retrieved fractional woody plant cover match those of % tree cover in the global MODIS Vegetation Continuous Fields product but also include shrubs. Good relationships were obtained with fractional shrub cover measured in pastures in the USDA, ARS Jornada Experimental Range but tree cover in higher elevation and riparian zones was dramatically overestimated as a result of the fixing of crown height and shape parameters. **Citation:** Chopping, M. J., L. Su, A. Laliberte, A. Rango, D. P. C. Peters, and J. V. Martonchik (2006), Mapping woody plant cover in desert grasslands using canopy reflectance modeling and MISR data, *Geophys. Res. Lett.*, *33*, L17402, doi:10.1029/2006GL027148.

1. Introduction

[2] Woody plants modify soils and microclimate in three major ways: C and N flux from soils increases; C and N pool sizes in plants and soils increases; and water use efficiency changes, with important implications for surface temperature and humidity at regional scales [*Huxman et al.*, 2005]. In addition, in many parts of the world woody shrubs are often invasive species and their proliferation has important economic implications through the loss of herbaceous productivity. In the United States, shrub encroachment has been severe, affecting over 8.7 million acres, or 84.1% of current and former U.S. grasslands [*Gori and Enquist*, 2003]. It is therefore important to map the distribution of woody plants in grass-dominated as well as in shrub-dominated zones. Simple geometric-optical (GO) models treat the surface as an assemblage of discrete objects of equal radius, shape and height, evenly distributed within a spatial unit. A tree or shrub crown is represented by a geometric primitive (e.g., spheroid, cone, or cylinder) whose center is located at a specified mean height above a (nominally diffuse scattering) background. These are 1-D models, i.e., they predict, independently for each mapped location, the top-of-canopy reflectance response to important canopy biophysical parameters (plant number density, foliage volume, mean canopy height and radius, and crown shape) as a linear combination of the contributions from sunlit and viewed and shaded and viewed components [*Li and Strahler*, 1985; *Chen et al.*, 2000], as in equation (1):

$$R = G.\,k_G + C.\,k_C + T.\,k_T + Z.\,k_Z \qquad (1)$$

where G, C, T, and Z are the "signatures", or contributions of the sunlit background, sunlit crown, shaded crown, and shaded background, respectively. The k_{GCTZ} are the proportions of these components in the instrument instantaneous field-of-view (IFOV). GO models are particularly appropriate for the exploitation of solar wavelength remote sensing data acquired at differing viewing and/or illumination angles because the proportions of sunlit and shaded crown and background in the IFOV vary with both viewing and illumination angles. However, special attention has to be paid to the use of GO models in arid and semi-arid environments because these have low leaf area per unit surface area, higher proportions of exposed, generally bright soil, and an important and highly variable understory cover of grasses, sub-shrubs, and/or forbs. In arid and semi-arid environments the background of soil and understory (including litter) can account for over 75% of fractional cover; it therefore usually determines brightness at the scale of a moderate resolution sensor ground-projected IFOV. Moreover, as a result of grazing history, hydrological setting and topo-edaphic variation, the background can be highly patchy and heterogeneous, leading to a wide range of canopy-background configurations. The major difficulty in inverting GO models in arid environments is whether the effects of relatively large plants (shrubs and trees) on the directional signal can be separated from those of the background.

2. Methods

[3] We used data from the Multiangle Imaging SpectroRadiometer (MISR) flown on NASA's Terra satellite over two study areas: the Jornada Experimental Range and the

[1]Department of Earth and Environmental Studies, Montclair State University, Montclair, New Jersey, USA.
[2]Agricultural Research Service, U.S. Department of Agriculture, Jornada Experimental Range, Las Cruces, New Mexico, USA.
[3]NASA Jet Propulsion Laboratory, Pasadena, California, USA.

0094-8276/06/2006GL027148$05.00

Sevilleta National Wildlife Refuge, located in southern and central New Mexico, respectively, and their environs. The total imaged area was over 3519 km^2 and all data were mapped to a 250 m grid. MISR consists of nine pushbroom cameras that acquire image data with nominal view zenith angles relative to the surface reference ellipsoid of 0.0°, 26.1°, 45.6°, 60.0°, and 70.5° in four spectral bands (446, 558, 672, and 866 nm). The 672 nm (red) band images are acquired with a nominal maximum crosstrack ground spatial resolution of 275 m in all nine cameras and all bands are acquired at this resolution in the nadir camera [*Diner et al.*, 1999]. Canopy-background configurations range from sparse young, small shrubs over a dark grassland matrix and older, larger plants over bright, sandy soils that can eventually become spatially contiguous. The dominant shrub species are honey mesquite (*Prosopis glandulosa*), creosotebush (*Larrea tridentate*), and tarbush (*Flourensia cernua*). The major tree species include cottonwood and salt-cedar in riparian environments and pinyon-juniper in the higher elevations.

[4] The simple geometric model (SGM) – a GO model incorporating a dynamic background and a volume scattering term – was used here [*Chopping et al.*, 2006a, 2006b]. It is formulated as equation (2):

$$R = G_{Walthall}(\vartheta_i, \vartheta_v, \varphi) \; . \; k_G(\vartheta_i, \vartheta_v, \varphi) + C_{Ross}(\vartheta_i, \vartheta_v, \varphi) \; . \; k_C(\vartheta_i, \vartheta_v, \varphi) \quad (2)$$

where ϑ_i, ϑ_v and φ are the view zenith, solar zenith and relative azimuth angles, respectively; k_G and k_C are the calculated proportions of sunlit and viewed background and crown, respectively; $G_{Walthall}$ is the background contribution from the Walthall model [*Walthall et al.*, 1985]; and C_{Ross} is the simplified Ross turbid medium approximation for plane parallel canopies [*Ross*, 1981]. The shaded components T and Z are discarded; they are assumed black. k_G and k_C are calculated exactly via Boolean geometry for the principal and perpendicular planes and approximated away from these; they are provided by equation (3) and equation (4), respectively:

$$k_G = \mathrm{e}^{-\lambda\pi r^2}\left\{\sec\vartheta_i' + \sec\vartheta_v' - O(\vartheta_i, \vartheta_v, \varphi)\right\} \quad (3)$$

$$k_C = \left(1 - \mathrm{e}^{-\lambda\pi r^2 \sec\vartheta_v'}\right)\frac{1}{2}(1 + \cos\varepsilon')$$
$$k_C = \left(1 - \mathrm{e}^{-\lambda\pi r^2 \sec\vartheta_v'}\right)\frac{1}{2}(1 + \cos\varepsilon') \quad (4)$$

where λ is the number density of objects; r is the average radius of these objects; and O is the overlap area between the shadows of illumination and viewing [*Wanner et al.*, 1995]; equation (5):

$$O = 1/\pi(t - \sin t \cos t)\left(\sec\vartheta_i' + \sec\vartheta_v'\right) \quad (5)$$

[5] These functions include the parameters b/r (vertical crown radius/horizontal crown radius) and h/b (height of crown center/vertical crown radius) which describe the shape and height of the crown. The prime indicates equivalent zenith angles obtained by a vertical scale transformation in order to treat spheroids as spheres (i.e., $\vartheta' = \tan^{-1}(b/r \tan\vartheta)$ [*Wanner et al.*, 1995]. ε' is the transformed scattering phase angle given by equation (6):

$$\cos\varepsilon' = \cos\vartheta_i'\cos\vartheta_v' + \sin\vartheta_i'\sin\vartheta_v'\cos\varphi \quad (6)$$

[6] The model's parameters are plant number density, mean crown radius, crown shape (b/r), crown center height (h/b), and leaf area index (LAI), where b and r are crown vertical and horizontal radii, respectively, and h is crown center height. The crown radius and number density parameters are coupled internally; identical results are obtained if the total crown area is maintained but either parameter is varied. In a similar way, the h/b and b/r parameters are coupled, since mean canopy height depends on b and the estimation of b depends on b/r. This implies that the model cannot be inverted to obtain both mean crown radius and plant number density simultaneously, or h/b and b/r simultaneously; however if number density is fixed then mean crown radius and therefore fractional cover can be obtained.

[7] To estimate the contribution of the background we used linear multiple regression on all three kernel weights (isotropic, *iso*; geometric, *geo*; and volume scattering, *vol*) of the semi-empirical LiSparse-RossThin BRDF model adjusted against MISR red band bidirectional reflectance factors (BRFs) in all nine cameras, plus the blue (B), green (G), and near-infrared (NIR) BRFs from the MISR *An* (nadir-viewing) camera. Relationships between *iso*, *geo*, and *vol* non-shrub mean grayscale level in Ikonos 1 m panchromatic imagery – a proxy for understory density – were approximately linear. Recovery of the relationship between soil/understory anisotropy and the kernel weights and B, G, and NIR BRFs, was accomplished for a range of canopy/background configurations (19 sites in the western part of the Jornada Experimental Range) by fixing mean shrub radius and number density extracted from 1 m panchromatic Ikonos imagery; fixing LAI, h/b and b/r model parameters at typical values (2.08, 2.00 and 0.20, respectively); and using an optimization algorithm to determine the Walthall model parameters providing the best fit, with the minimum of the Root Mean Square Error (RMSE) with respect to MISR red band data in all nine views adopted as the merit function. This allowed regression of each of the four Walthall model parameters on the six independent variables. Initial tests of this approach by modeling MISR data over a 5 km^2 area were reasonably successful ($R^2 = 0.78$, RMSE = 0.013, N = 3969 [*Chopping et al.*, 2006a]). Experiments using the Compact High Resolution Imaging Spectroradiometer on the European Space Agency's Proba-1 platform produced similar results [*Chopping et al.*, 2006b].

[8] To invert the model the SGM was adjusted against the MISR data by means of numerical optimization, for each mapped location. Forward differencing was used for estimates of partial derivatives of the objective function and a Newton search method was used at each iteration to decide which direction to pursue in the parameter space. The objective function was min(|RMSE|) with no weighting of the error terms. Only mean shrub radius was left as a free parameter, with other parameters set to the same typical values specified above. No constraints were imposed. Retrievals were thus effectively for fractional woody plant cover, a function of plant number density and mean radius.

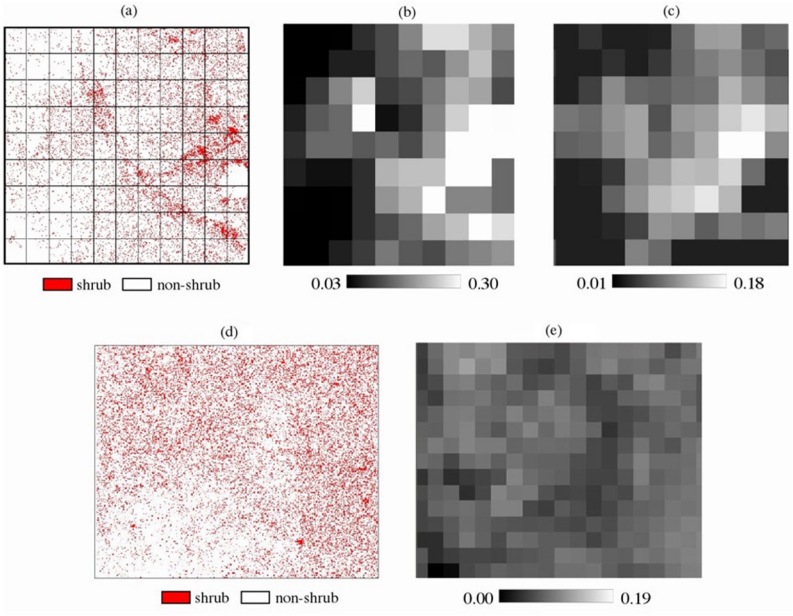

Figure 1. (a) Shrub map for parts of pasture 12 in the Jornada from segmentation of QuickBird (QB) imagery (b) shrub cover calculated from Figure 1a and aggregated to 250 m (c) shrub cover retrieved using MISR/SGM (d) QB shrub map for parts of pastures 8/9 in the Jornada (e) corresponding map from MISR/SGM. Pasture locations are indicated in Figure 3d.

We applied this method for the areas encompassing the Jornada Experimental Range and the Sevilleta National Wildlife Refuge and assessed the results against shrub cover estimates derived from high resolution QuickBird and Ikonos imagery [*Laliberte et al.*, 2004]. We also compared distributions against those in the MODIS Vegetation Continuous Fields (VCF) % tree cover maps [*Hansen et al.*, 2003].

3. Results and Discussion

[9] The results show that the method allows a partial separation of the upper canopy and background contributions. When used to predict fractional shrub cover for part of pasture 12 in the Jornada Experimental Range, ~10 kilometers from the area used for calibration of the background and for which independent estimates were available, the distributions exhibited a good match and an R^2 of 0.47 was obtained (Figure 1). The reference data were derived from precision shrub maps obtained using image segmentation techniques applied to 0.6 m QuickBird panchromatic images. A good match was also found in imagery for parts of pastures 8 and 9 (Figures 1d and 1e). There is a bias in the predicted cover estimates for pasture 12 (Figure 2a) that is improved only slightly if the SGM is modified so that the contribution from volume scattering is not weighted by the fraction of sunlit and viewed shrub canopy in the IFOV, k_C (Figure 2b).

[10] In addition to shrubs, the maps for the Jornada Experimental Range and the Sevilleta National Wildlife Refuge and their environs include pinyon-juniper woodlands on the San Andres mountains (to the east of the Jornada), and in other elevated areas (e.g., Summerford Mountain, the small bright feature in the southwest quadrant of the Jornada map); oneseed juniper woodlands (to the east of the Sevilleta); and cottonwood and tamarisk trees in the

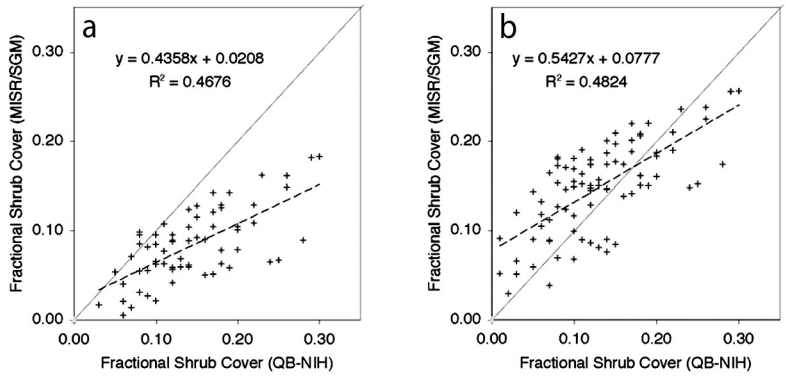

Figure 2. Retrieved vs. measured shrub cover (a) SGM (b) SGM with k_C = 1.00. QB-NIH refers to QuickBird-derived maps from which cover was calculated using US the National Institutes of Health *Image* package.

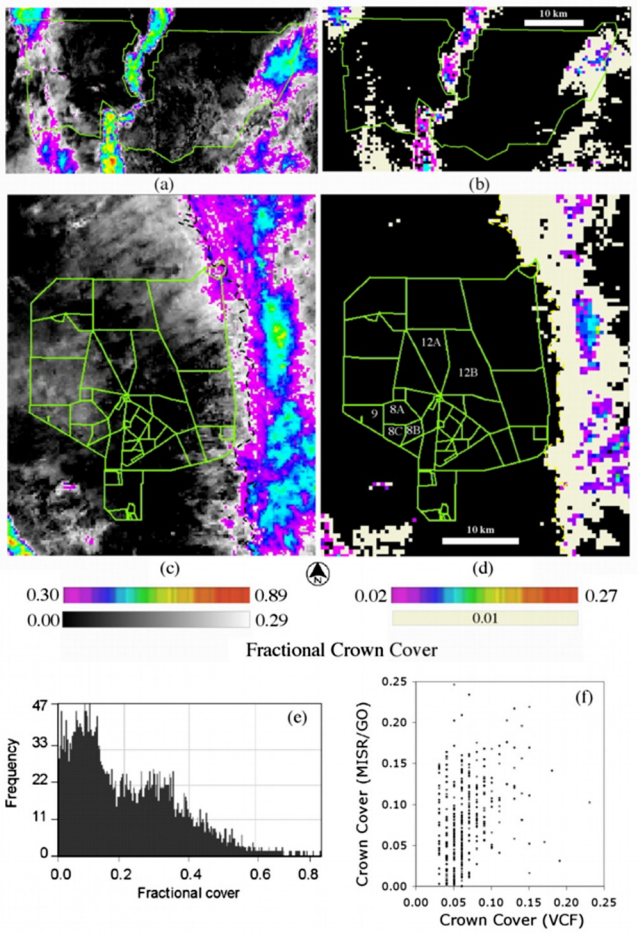

Figure 3. Woody plant cover map obtained by adjusting the SGM GO model against MISR red band data (a) in the Sevilleta National Wildlife Refuge (b) MODIS VCF % tree cover map for the Sevilleta (c) in the Jornada Experimental Range, dotted line is the tree-shrub boundary from the VCF map (d) MODIS VCF % tree cover map for the Jornada (e) frequency distribution for the Jornada fractional cover map, excluding zero (f) scatterplot showing the relationship between the two data sets (see text). The solid green lines in Figures 3a and 3c indicate the boundaries of the Sevilleta and fencelines in the Jornada.

riparian environments of the Rio Grande (in the SW quadrant of the Jornada map and the center of the Sevilleta map). Within shrub-dominated areas the range of retrieved fractional cover values is very reasonable (0.01–0.20) but in the higher-elevation woodland areas, cover is dramatically over-estimated: the brightest locations in the maps correspond to values of up to ~0.90. However, the spatial distributions compare well with those of tree cover in the VCF % tree cover maps (Figure 3). Note that the VCF map includes only tree cover and is derived using phenological and spectral reflectance metrics, whereas the MISR/GO-derived map includes all large woody plants as it is based on exploiting the information on canopy structure encapsulated in the MISR data: the inversion algorithm is attempting to match not only brightness but also the (mostly bell) shapes of the MISR zenithal profiles. The frequency distribution for the Jornada fractional cover map (Figure 3e) is bi-modal, with peaks at ~0.10 and ~0.30 and a division between shrub and tree canopies at ~0.25. Although there are likely to be locations where shrub cover exceeds this and tree cover is lower than this, the line defined by this value closely corresponds to the tree/no-tree boundary in the VCF map (Figure 3c). There are many locations in both the Jornada and the Sevilleta for which the inversion algorithm failed, usually because the background was predicted to be too dark to allow any increase in shrub cover above zero. These were assigned values of zero. Inspection of many high resolution Ikonos 1 m resolution panchromatic images showed that shrub cover is quite low in these areas (Figure 4). Bias in the cover estimates may be the result of the use of incorrect crown radius and number density estimates owing to spatial contiguity in shrub maps derived from high resolution imagery, fixing the crown height and shape parameters, or model inadequacies.

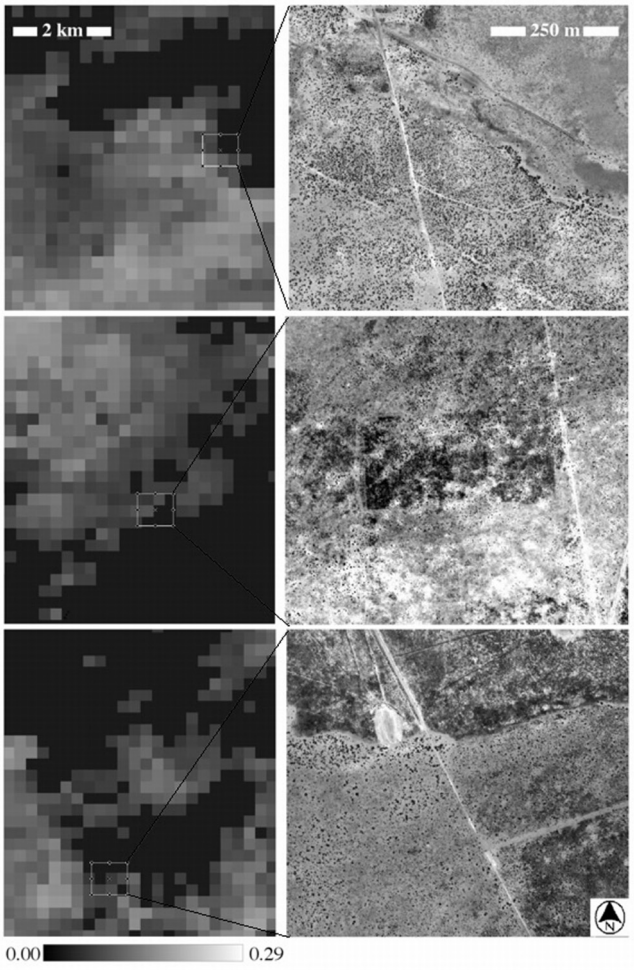

Figure 4. (left) Subsets of the MISR/SGM fractional shrub cover map for the Jornada Experimental Range including areas (in black) where inversion failed owing to very sparse shrub cover. (right) Ikonos 1 m pan imagery shown with a 2-standard deviation stretch. Large shrubs appears as dots; dense understory and grasses generally appear darker. Ikonos satellite imagery courtesy of GeoEye. Copyright 2006. All rights reserved.

[11] Following resampling of the MISR/GO data to the 500 m VCF map grid, a correlation coefficient of 0.55 was obtained between the data sets, with a RMSE of 0.22. Note that the VCF estimates are also subject to error: *White et al.* [2005] found that in the southwest US VCF has a positive bias for low tree cover and a negative bias for high tree cover (at > = 60% cover, VCF is up to 45% too low with respect to data from 3954 ground plots, respectively). If the retrieved fractional cover estimates for trees only (meeting the criteria VCF > 0.02 and retrieved cover > = 0.3) are scaled with cover′ = cover/2.0 − 0.2, the correlation coefficient is only 0.32, even though a quasi-linear relationship is evident (Figure 3f). This is probably at least partly owing to quantization effects and misregistration between the maps.

4. Conclusions

[12] This study demonstrates the potential of monospectral, multi-angle data for estimating the abundance of woody plants over large areas. Using the weights of Li-Ross kernel-driven BRDF model to estimate the soil/understory background contribution and numerical optimization to retrieve mean shrub radius is an effective approach for the mapping of fractional shrub cover at large scales using simple GO models. Estimates of fractional woody plant cover made some distance from the sites used for calibrating the background contribution showed a robust, if biased, relationship to measurements. Estimates were much higher than they should have been for the woodland areas in the higher elevations and riparian zones mainly because the shape and height parameters of the GO model were fixed at typical values for shrubs. We recognize that is not reasonable to use the same fixed model parameters governing height and shape for areas with both shrubs and trees, since trees are taller, larger objects with more prolate crowns and therefore cause a greater proportion of the background to be shaded than the same area occupied by an equivalent cover of shrubs. Additional work is required to determine whether allowing adjustable model crown height and/or shape parameters is feasible without compromising inversions. Considering the remotely sensed signal to comprise contributions from large plants and a soil/understory background represents a different paradigm to that adopted in most remote sensing of vegetation, where the separation is made in the spectral domain and soil and vegetation are considered as the components; here the separation is made by accessing structural information, since the directional signal results mainly from shadowing by protrusions (shurbs and trees) and scattering by facets (leaves).

[13] **Acknowledgments.** The MISR data were obtained from the NASA Langley Research Center Atmospheric Science Data Center. We thank Matt Smith (Global Land Cover Facility, University of Maryland, College Park, MD), and Mike Friggens and Greg Shore (Sevilleta LTER, Albuquerque, NM). This research was supported by NASA Earth Observing System grant to MC (NNG04GK91G). The Jornada Experimental Range is administered by the USDA Agricultural Research Service and is a Long Term Ecological Research site supported by the National Science Foundation (DEB 0080412). The Sevilleta National Wildlife Refuge is administered by the U.S. Fish and Wildlife Service. This research is partly supported by a National Science Foundation grant to the University of New Mexico (DEB 0080529) and to New Mexico State University (DBI-9896218).

References

Chen, J. M., X. Li, T. Nilson, and A. Strahler (2000), Recent advances in geometrical optical modelling and its applications, *Remote Sens. Rev.*, *18*, 227–262.

Chopping, M., L. Su, A. Rango, J. V. Martonchik, D. P. C. Peters, and A. Laliberte (2006a), Remote sensing of woody shrub cover in desert grasslands using MISR with a geometric-optical canopy reflectance model, *Remote Sens. Environ.*, in press.

Chopping, M., L. Su, A. Laliberte, A. Rango, D. P. C. Peters, and N. Kollikkathara (2006b), Mapping shrub abundance in desert grasslands using geometric-optical modeling and multiangle remote sensing with CHRIS/Proba, *Remote Sens. Environ.*, *104*(1), 62–73, doi:10.1016/j.rse.2006.04.022.

Diner, D. J., G. P. Asner, R. Davies, Y. Knyazikhin, J.-P. Muller, A. W. Nolin, B. Pinty, C. B. Schaaf, and J. Stroeve (1999), New directions in Earth observing: Scientific applications of multi-angle remote sensing, *Bull. Am. Meteorol. Soc.*, *80*(11), 2209–2229.

Gori, D. F., and C. A. F. Enquist (2003), An assessment of the spatial extent and condition of grasslands in central and southern Arizona, southwestern New Mexico and northern Mexico, report, 28 pp. Ariz. Chap., Nature Conserv., Tucson.

Hansen, M. C., R. Defries, J. Townshend, M. Carroll, C. Dimiceli, and R. Sohlberg (2003), Global percent tree cover at a spatial resolution of 500 meters: First results of the MODIS vegetation continuous fields algorithm, *Earth Inter.*, *7*(10), 1–15.

Huxman, T. E., B. P. Wilcox, D. D. Breshears, R. L. Scott, K. A. Snyder, E. E. Small, K. Hultine, W. T. Pockman, and R. B. Jackson (2005), Ecohydrological implications of woody plant encroachment, *Ecology*, *86*(2), 308–319.

Laliberte, A. S., A. Rango, K. M. Havstad, J. F. Paris, R. F. Beck, R. McNeely, and A. L. Gonzalez (2004), Object-oriented image analysis for mapping shrub encroachment from 1937 to 2003 in southern New Mexico, *Remote Sens. Environ.*, *93*, 198–210.

Li, X., and A. H. Strahler (1985), Geometric-optical modeling of a conifer forest canopy, *IEEE Trans. Geosci. Remote Sens.*, *23*, 705–721.

Ross, J. K. (1981), *The Radiation Regime and Architecture of Plant Stands*, 392 pp., Springer, New York.

Walthall, C. L., et al. (1985), Simple equation to approximate the bidirectional reflectance from vegetative canopies and bare surfaces, *Appl. Opt.*, *24*, 383–387.

Wanner, W., X. Li, and A. H. Strahler (1995), On the derivation of kernels for kernel-driven models of bidirectional reflectance, *J. Geophys. Res.*, *100*, 21,077–21,090.

White, M. A., J. D. Shaw, and R. D. Ramsey (2005), Accuracy assessment of the vegetation continuous field tree cover product using 3954 ground plots in the south-western USA, *Int. J. Remote Sens.*, *26*(12), 2699–2704.

M. J. Chopping and L. Su, Department of Earth and Environmental Studies, Montclair State University, Montclair, NJ 07043, USA. (choppingm@pegasus.montclair.edu)

A. Laliberte, D. P. C. Peters, and A. Rango, Agricultural Research Service, USDA, Jornada Experimental Range, P.O. Box 30003, Las Cruces, NM 88003, USA.

J. V. Martonchik, NASA Jet Propulsion Laboratory, 4800 Oak Grove Drive, Pasadena, CA 91109, USA.